

Negative Complexity of Formation: the Compact Dimensions Strike Back

Netta Engelhardt and Åsmund Folkestad

*Center for Theoretical Physics, Massachusetts Institute of Technology,
Cambridge, MA 02139, USA*

engeln@mit.edu, afolkest@mit.edu

ABSTRACT: We show that the vacuum-subtracted maximal volume, the proposed holographic dual to complexity of formation, can be negative when contributions from compact directions are included. We construct explicit solutions with arbitrarily negative complexity of formation in asymptotically $\text{AdS}_4 \times S^7$ SUGRA. These examples rely critically on the compact directions, specifically the fact that the full eleven-dimensional spacetime is not asymptotically AdS_{11} . While there is some ambiguity in the extension of the holographic complexity proposal to the compact directions, we show that the two natural candidates can both have arbitrarily negative complexity of formation in SUGRA solutions. We further find examples in which complexity can even *decrease* at late times, including cases of both single-sided geometries and two-sided wormholes. In particular, we construct a cosmological wormhole with simultaneously negative and decreasing complexity of formation (as computed by volume) at late times. We find a distinguished role for relevant primaries in these constructions and comment on possible interpretations.

Contents

1	Introduction	1
2	Lower Unbounded \mathcal{C}_F in SUGRA	5
3	Negatively Divergent \mathcal{C}_F	11
3.1	AdS Vacuum Decay	11
3.2	Decaying Cosmological Wormholes	15
A	Appendix	17
A.1	The DEC and SEC in type II and $D = 11$ SUGRA	17
A.2	General properties of $K = 0$ slices in SUGRA	20
A.3	AdS Vacuum Decay Computations	21

1 Introduction

Recent progress on the emergence of spacetime has crucially relied on the geometrization of quantum information theoretic quantities [1–16]. A relative newcomer to this set of connections has been the geometrization of computational complexity [11–14], either through the proposed Complexity=Action [13, 14] or Complexity=Volume duality [12]. The latter, which is our focus in this article, relates the circuit complexity \mathcal{C} of a given holographic CFT_d state $|\psi(\tau)\rangle$ relative to some reference state $|R\rangle$ to regulated bulk spatial volumes:

$$\mathcal{C}(|\psi(\tau)\rangle, |R\rangle) = \max_{\Sigma} \frac{\text{vol}[\Sigma]}{G_N L} \equiv \mathcal{C}_V(|\psi(\tau)\rangle), \quad (1.1)$$

where Σ a bulk hypersurface that intersects the conformal boundary on the timeslice τ ; L is a length scale which we will take to be the AdS radius, and \mathcal{C}_V a convenient shorthand for the gravitational quantity.

In a recent paper [17], we proved that the *complexity of formation* \mathcal{C}_F [14, 18] satisfies

$$\mathcal{C}_F(|\psi\rangle) \equiv \mathcal{C}_V(|\psi\rangle) - \mathcal{C}_V(|0\rangle) \geq 0, \quad (1.2)$$

with equality if and only if $|\psi\rangle = |0\rangle$, where $|0\rangle$ is the vacuum dual to pure AdS_{d+1} . We established this for asymptotically AdS_{d+1} spacetimes under the assumption of the weak curvature condition (WCC):

$$t^a t^b \left(R_{ab} - \frac{1}{2} g_{ab} R - \frac{d(d-1)}{L^2} g_{ab} \right) \geq 0, \quad \forall \text{ timelike } t^a, \quad (1.3)$$

which in Einstein gravity reduces to the weak energy condition (WEC): $T_{ab} t^a t^b \geq 0$ for all timelike t^a . The result (1.2) implies that among the states with a classical asymptotically AdS_{d+1} dual respecting the WCC, the vacuum is the least \mathcal{C}_V -complex. That is, WCC-respecting excitations of the vacuum move away from the reference state as measured by the complexity. The necessity of the WCC is clear from [19, 20], who found examples in which the vacuum-subtracted volume is negative; in those examples the WCC is violated.

The assumption of the WCC is somewhat unnatural from a holographic perspective: consistency conditions in the large- N , large- λ limit of the AdS/CFT correspondence are typically proven using the Null Curvature Condition (NCC) $R_{ab} k^a k^b \geq 0$ for null vectors k^a . The latter (strictly weaker) condition is expected to be true for any valid classical matter; the same, however, is not true for the WCC [21]. Nevertheless, it turns out that the WCC holds in type II and eleven-dimensional SUGRA (see appendix A.1): even though the dimensional reduction of an asymptotically $\text{AdS}_{d+1} \times K$ over the compact dimensions K may violate the WCC while satisfying the NCC, inclusion of the compact dimensions restores the WCC. Prima facie, then, it may be tempting to conclude that when working in full ten or eleven dimensional SUGRA, our results immediately imply that complexity of formation is *always* positive. It would then be natural to conclude that $\mathcal{C}(|\psi\rangle, |R\rangle)$ should be identified with $\mathcal{C}_F(|\psi\rangle)$, with a reference state $|R\rangle$ that is identically the vacuum $|0\rangle$.

This naive conclusion, however, suffers from several flaws. First, the Complexity=Volume proposal does not admit an obvious generalization allowing the inclusion of compact directions. There are (at least) two natural candidates: (1) the volume of the maximal volume slice Σ_{full} in the full $\text{AdS}_{d+1} \times K$ spacetime; or (2) the volume of the maximal volume slice Σ_{reduced} extended in the non-compact directions. It is simple (see Sec. 2) to show that in general the dimensional reduction of Σ_{full} does not result in Σ_{reduced} , and that consequently

$$\text{vol}[\Sigma_{\text{full}}] \neq \text{vol}[\Sigma_{\text{reduced}} \times K].$$

A maximal volume slice in the full spacetime need not be maximal in the AdS directions, and vice versa.

Our goal here, however, will not be to argue in favor of either (1) or (2) but to demonstrate that *neither* candidate can avoid a negative complexity of formation: the WCC restoration that accompanies the inclusion of compact directions fails to save either candidate from predicting that certain valid spacetimes in AdS/CFT are simpler than the vacuum¹. As a consequence, since \mathcal{C}_F is not positive semi-definite, it cannot be reinterpreted as the complexity with the vacuum as the reference state. To simplify matters, we will demonstrate this in a special case where the two candidate proposals coincide: a moment of time symmetry. In such a case, Σ_{full} reduces in the AdS directions to Σ_{reduced} , so that any conclusions are free of ambiguities relating to a choice between (1) and (2).

This result may at first appear to contradict our proof in [17]. How can the vacuum-subtracted maximal volume be negative in spacetimes respecting the WCC? The answer is a prime realization of the principle of conservation of misery: while the inclusion of compact directions restores the WCC, it in turn violates our assumption about AdS_{d+1} asymptotics. Thus we have two (mutually exclusive) options: accept violations of WCC in the absence of compact directions, or accept violations of AdS_{d+1} asymptotics. As it turns out, either option leads to states with negative complexity of formation.

In the following, we find a family of AdS_4 initial data supported by scalar tachyons above the Breitenlohner-Freedman bound [22], inherited from a truncation and dimensional reduction over the compact directions of eleven-dimensional SUGRA. In the full asymptotically $\text{AdS}_4 \times S^7$ data, the WCC is satisfied, but upon dimensional reduction the resulting spacetimes violate the WCC and satisfy the NCC. These geometries come in two flavors²: with and without boundary sources. For the former, the inclusion of boundary sources yields asymptotically AdS_4 spacetimes undergoing AdS false vacuum decay; such spacetimes, again supported by scalar tachyons, have a negatively divergent complexity of formation that decreases at late times. Among these spacetimes is a novel cosmological wormhole; even though the spacetime connects two asymptotic boundaries (with no dS region in between [25]), we find that the holographic volume complexity is nevertheless *smaller* than that of pure AdS. While spacetimes with negative and divergent \mathcal{C}_F due to boundary sources were previously considered by [26],

¹By ‘valid’ here we mean a stricter definition than is typically used (which is often just the requirement of the NEC and global hyperbolicity: here we mean that they are inherited from top down truncations of SUGRA).

²For computational facility, the examples with boundary sources are not constructed in an exact dimensional reduction of eleven-dimensional SUGRA, but instead with a slightly modified (but qualitatively similar) scalar potential, which enables analytical solutions. Analogous one-sided spacetimes were considered in $D = 11$ SUGRA reduced to $\text{AdS}_4 \times S^7$ in [23, 24], and we expect all of our qualitative findings in Sec. 3 to apply in $D = 11$ SUGRA.

our examples without boundary sources are quite distinct, and should be regarded as the main finding of this paper (although we also expand on examples with boundary sources, more analogous to the ones discussed in [26]). In this case we find initial data with arbitrarily negative (but finite) complexity of formation, both when viewed in eleven and four dimensions. The arbitrarily low complexity in this case is not caused by altering the boundary theory. Instead, it is obtained by a smooth deformation of the CFT state away from vacuum, and the low \mathcal{C}_V is a genuine IR-effect caused by the compact dimensions.

There is however an underlying common denominator to all of our examples: they are constructed by turning on relevant scalar primaries in the CFT. This pattern together with the theorems of [17] suggests potential insights into the landscape of low complexity holographic states. If tachyonic bulk scalars, which are dual to relevant CFT scalar primaries, happen to be the only WEC-violating fields, then the only way to reduce the “distance” – as measured by \mathcal{C}_V – to $|R\rangle$ below the fixed nonzero value $\mathcal{C}_V(|0\rangle)$ is to turn on VEVs for relevant scalars. Other operators will be dual to WEC-respecting fields, and so turning them on will cause \mathcal{C}_V to increase with respect to the vacuum value. Thus, the presence of unstable directions of the IR fixed point correlates with the possibility of reducing complexity below the vacuum value. This could be due to the fact that the vacuum of a potential gapped phase at the end of the RG flow has significantly fewer correlations, simplifying the preparation of the state.

Our particular examples of low complexity spacetimes also provide potential insight into the reference state $|R\rangle$ implicit in the CV proposal. These examples are constructed by creating pockets of approximately constant scalar field at a moment of time-symmetry in the bulk, resulting in an effective AdS radius smaller than the asymptotic value L within the pocket. We find that \mathcal{C}_F becomes arbitrarily negative as the pocket becomes larger: that is, the complexity becomes progressively closer to that of $|R\rangle$ via this reduction of the effective AdS radius in an increasingly large region. Since the limit of small AdS radius is not a well-defined classical geometry, this finding is consistent with the common perspective that $|R\rangle$ is a state without a geometric dual, e.g. a set of factorized qubits.

What is the upshot of our results for the Complexity=Volume proposal? At minimum, there is need for an unambiguous prescription that accounts for contributions from compact dimensions. It is clear that volumes can have a qualitatively different behavior when compact dimensions are included. On a more speculative level, there appears to be a sharp distinction (in the dimensionally-reduced picture) between operators whose dual is WCC-respecting and WCC-violating; acting on the vacuum with the former can only increase complexity; the latter, however, can decrease complexity. It would be interesting to understand this better in the dual CFT, perhaps using the

proposed definitions of complexity in [27–30].

The paper is structured as follows. In Sec. 2 we present our SUGRA maximal volume asymptotically $\text{AdS}_4 \times S^7$ initial data, together with its dimensional reduction. Then, to ensure that our constructed initial data gives the unique maximal volume slice in the evolved spacetime, we derive general properties of maximal volume slices in type II and $D = 11$ SUGRA in Sec. A.2. Finally, in Sec. 3 we turn on boundary sources to study spacetimes undergoing AdS vacuum decay, both one-sided and two-sided. The appendix A provides technical details omitted in the main text.

2 Lower Unbounded \mathcal{C}_F in SUGRA

We begin by constructing asymptotically $\text{AdS}_4 \times S^7$ examples with negative complexity of formation supported by a well-studied truncation of eleven-dimensional SUGRA compactified on the S^7 [31]³

$$S = \frac{1}{8\pi G_N} \int_M d^4x \sqrt{-g} \left[\frac{1}{2}R + \frac{3}{L^2} - \frac{1}{2}(\nabla\phi)^2 - V(\phi) \right], \quad (2.1)$$

with scalar potential

$$V(\phi) = \frac{1}{L^2} \left(1 - \cosh \sqrt{2}\phi \right). \quad (2.2)$$

Since $V(\phi)$ is unbounded below, this theory violates the WEC (and equivalently the WCC). However, it is simple to check that the tachyonic scalar mass about the $\phi = 0$ vacuum is above the BF bound. Furthermore, the null energy condition is satisfied, as always is the case for minimally coupled scalars.

A solution to the equations of motion of (2.1) with four-dimensional line element ds_4^2 lifts to a solution of eleven dimensional SUGRA with geometry

$$ds^2 = \Delta^{2/3} ds_4^2 + \frac{4L^2}{\Delta^{1/3}} \sum_{i=1}^4 X_i^{-1} (d\mu_i^2 + \mu_i^2 d\psi_i^2), \quad (2.3)$$

³This theory was used to construct big crunch geometries in [23, 24]. Our boundary conditions will differ from [23, 24], so that the boundary dual will be different. The spacetimes in the next section will more closely resemble the situation in [23, 24].

where ds_4^2 is the four-dimensional metric and

$$\begin{aligned}
\mu_i &= (\sin \theta, \cos \theta \sin \varphi, \cos \theta \cos \varphi \sin \xi, \cos \theta \cos \varphi \cos \xi), \\
X &\equiv X_1 = X_2 = e^{-\frac{\phi}{\sqrt{2}}}, \\
X_3 &= X_4 = X^{-1}, \\
\Delta &= \sum_{i=1}^4 X_i \mu_i^2.
\end{aligned} \tag{2.4}$$

The angles $(\theta, \varphi, \psi_1, \psi_2, \psi_3, \psi_4)$ run over the range $[0, \pi]$, while $\xi \in [0, 2\pi)$. If we set $\phi = 0$ ($X_i = 1$), then the transverse space just becomes a round S^7 with radius $2L$: turning on the scalar ϕ squashes the S^7 .

We now want to construct initial data on a spherically symmetric maximal volume slice Σ which has arbitrarily low complexity of formation in the $(d+1) = 4$ theory (2.1). Furthermore, upon success of this endeavor, we want to investigate whether considering the full volume in eleven-dimensional SUGRA restores positivity or boundedness from below. Let us first note that in the spherically symmetric case, if Σ has embedding coordinates $(t(r), r, \Omega_i)$ where Ω_i are the angles on the 2-sphere, then Σ can be lifted to a slice $\tilde{\Sigma}$ in the eleven-dimensional spacetime with embedding coordinates $(t(r), r, \Omega_i, \theta, \varphi, \xi, \psi_i)$. However, the slice $\tilde{\Sigma}$ is generally not a maximal volume slice (even though Σ is): turning on the scalar ϕ induces volume in the compact dimensions, so if $\partial_t \phi \neq 0$ on Σ , then we can gain volume in the eleven-dimensional spacetime (\tilde{M}, \tilde{g}) by deforming $\tilde{\Sigma}$. However, letting K_{ab} denote the extrinsic curvature, if we take a moment of time symmetry, $K_{ab}[\Sigma] = \partial_t \phi = 0$, then we will also be at a moment of time-symmetry in eleven dimensions, and so $\tilde{\Sigma}$ is also extremal in (\tilde{M}, \tilde{g}) .

In a moment we will construct explicit initial data, but let us first find an expression for the volume of $\tilde{\Sigma}$. We can take our coordinates on Σ so that

$$\begin{aligned}
ds^2|_{\Sigma} &= B(r)dr^2 + r^2 d\Omega^2, \\
ds^2|_{\tilde{\Sigma}} &= \Delta^{2/3} (B(r)dr^2 + r^2 d\Omega^2) + \frac{4L^2}{\Delta^{1/3}} \sum_{i=1}^4 X_i^{-1} (d\mu_i^2 + \mu_i^2 d\psi_i^2),
\end{aligned} \tag{2.5}$$

for some $B(r) > 0$. Integrating out the compact dimensions, we find an effective volume form $\tilde{\epsilon}$ on Σ :

$$\tilde{\epsilon} = (2L)^7 f \left(e^{-\frac{\phi}{\sqrt{2}}} \right) \epsilon, \tag{2.6}$$

where ϵ is the canonical volume form on Σ induced in the four-dimensional spacetime (M, g) and

$$f(X) = \pi^4 \frac{9(1 + X^{2/3})(2 + 4X^{2/3} + 8X^{4/3} + 7X^2 + 8X^{8/3} + 4X^{10/3} + 2X^4)}{70X^{1/3}(1 + X^{2/3} + X^{4/3})^3}. \tag{2.7}$$

When $\tilde{\epsilon}$ is integrated over Σ , it gives the volume of $\tilde{\Sigma}$. Since $f(X) \geq f(1) = \text{vol}[S^7]$, including the compact dimensions always increases the volume compared to the naive multiplication of the $d = 3$ volume with $(2L)^7 \text{vol}[S^7]$. For large $|\phi|$, to leading order

$$\tilde{\epsilon} = \frac{27}{35} (2L)^7 \text{vol}[S^7] e^{\frac{|\phi|}{3\sqrt{2}}} \epsilon. \quad (2.8)$$

Thus, for large scalar condensates there is generally an *exponential* difference in $|\phi|$ between the naive $(2L)^7 \text{vol}[S^7] \text{vol}[\Sigma]$ and the true volume $\text{vol}[\tilde{\Sigma}]$. This clearly demonstrates that compact directions can dramatically modify the volume even if the extremal slice is unchanged.

We now want to pick initial data leveraging the negativity of $V(\phi)$ to minimize the volume of Σ . The solution of the constraint equations for Einstein-Maxwell-Scalar theory on a spherically symmetric maximal volume slice at a moment of time symmetry and with $d = 3$ is [17]

$$\begin{aligned} B(r) &= \left(1 + r^2 - \frac{\omega(r)}{r} \right)^{-1}, \\ \omega(r) &= \frac{1}{2} \int_0^r d\rho \rho^2 e^{\frac{1}{2} \int_r^\rho dz \phi'(z)^2} \left[(1 + \rho^2) \phi'(\rho)^2 + 2 - 2 \cosh \sqrt{2} \phi \right], \end{aligned} \quad (2.9)$$

where we pick units of $L = 1$ for brevity. The quantity $\omega(r)$ is a quasi-local mass function, and $\omega(\infty)$ is proportional to the conserved spacetime mass when $\omega(\infty)$ is finite [23].

We now pick the scalar profile on Σ to fall off in such a way so that the evolution of the initial data on Σ does not spoil the AdS asymptotics. Furthermore, we must ensure that $B(r) > 0$ everywhere so that Σ is everywhere spacelike. Beyond these two constraints, we are free to choose the profile for ϕ .⁴ The usual near boundary analysis of the Einstein-Klein-Gordon system constrains the asymptotic behavior of ϕ :

$$\phi(r, x) = r^{-\Delta_-} \left(\phi^{(0)}(x) + \phi^{(2)}(x) r^{-2} + \dots \right) + r^{-\Delta_+} \left(\psi^{(0)}(x) + \psi^{(2)}(x) r^{-2} + \dots \right), \quad (2.10)$$

⁴We do not have a guarantee that it is possible to prepare (2.11) via the Euclidean path integral. However, for our conclusions to fail, it would have to be impossible to construct any qualitatively similar scalar condensate at a moment of time symmetry, since our findings do not depend on the particular quantitative details of the condensate (2.11). Any tachyonic scalar condensate should give the same conclusion as long as we have (1) a pocket where ϕ is non-zero and approximately constant, (2) the pocket is of size at least $r \sim L$, and (3) the scalar falls off as slowly as is consistent (2.10) and finite energy. It seems unlikely that such profiles cannot be prepared. In fact, [32] shows perturbatively that such profiles can be prepared using the Euclidean path integral.

where $\Delta_- = 1$ and $\Delta_+ = 2$. In order to avoid turning on boundary sources and to keep $\omega(\infty)$ finite (so the volume divergence structure agrees with that of pure AdS and so the Balasubramanian-Kraus stress tensor is defined [33]), we take $\phi^{(2n)} = 0$.

Let us construct one-sided initial data with no minimal surfaces, so that one coordinate patch covers the whole of Σ (this happens when $B(r)$ is nowhere divergent [17]). We choose the profile

$$\phi(r) = 1 - e^{-a^2/r^2}, \quad (2.11)$$

which has the requisite $\mathcal{O}(r^{-2})$ behavior needed to keep $\omega(\infty)$ finite. In the appendix we prove that in type II and $D = 11$ SUGRA, (1) any $K = 0$ slice is maximal, and (2) there can only be one maximal slice at a fixed anchoring. Thus, the spacetime obtained by evolving our initial data cannot possess another maximum volume slice with larger volume.

It can be checked that the profile (2.11) results in $0 < B(r) < \infty$, so that our assumption of no minimal surfaces is satisfied. We now proceed to calculate volumes of Σ and $\tilde{\Sigma}$ relative a constant- t slice of AdS_4 and $\text{AdS}_4 \times S^7$, respectively:

$$\begin{aligned} \Delta V_{\Sigma}(a) &= \text{vol}[S^2] \int_0^\infty dr r^2 \left[\frac{1}{\sqrt{1+r^2 - \frac{\omega(r)}{r}}} - \frac{1}{\sqrt{1+r^2}} \right], \\ \Delta V_{\tilde{\Sigma}}(a) &= \text{vol}[S^2] 2^7 \int_0^\infty dr r^2 \left[\frac{f\left(e^{-\frac{\phi}{\sqrt{2}}}\right)}{\sqrt{1+r^2 - \frac{\omega(r)}{r}}} - \frac{\text{vol}[S^7]}{\sqrt{1+r^2}} \right], \end{aligned} \quad (2.12)$$

(Here the factor 2^7 appears since the round S^7 has radius 2 in units of $L = 1$.)

In Fig. 1 we plot the result: we show ΔV_{Σ} and $\Delta V_{\tilde{\Sigma}}/V(S^7)2^7$ plotted against a , together with the profile $\omega(r)$ for the value $a = 5$. Other values of a give a qualitatively similar shape for $\omega(r)$. We see that the vacuum subtracted volume for Σ becomes negative as we increase a . We find no signs of this decrease stopping for very large values of a . However, if we impose a finite cutoff at $r \sim \frac{1}{\epsilon}$, the decrease will saturate at $a \sim 1/\epsilon$. Either way, we see that turning on an increasingly large condensate of our tachyonic scalar field (or in the CFT language, turning on an increasingly large VEV for a relevant scalar primary) takes us closer to the reference state $|R\rangle$. This is a very distinct behavior which a CFT dual to volume ought to reproduce.

What is the bulk mechanism leveraged in these examples that allow negative \mathcal{C}_F ? In the WEC-violating case ($d = 3$) it is the absence of a lower bound on the intrinsic Ricci scalar of maximal volume slices. It is illustrative to look at a conjecture of Schoen

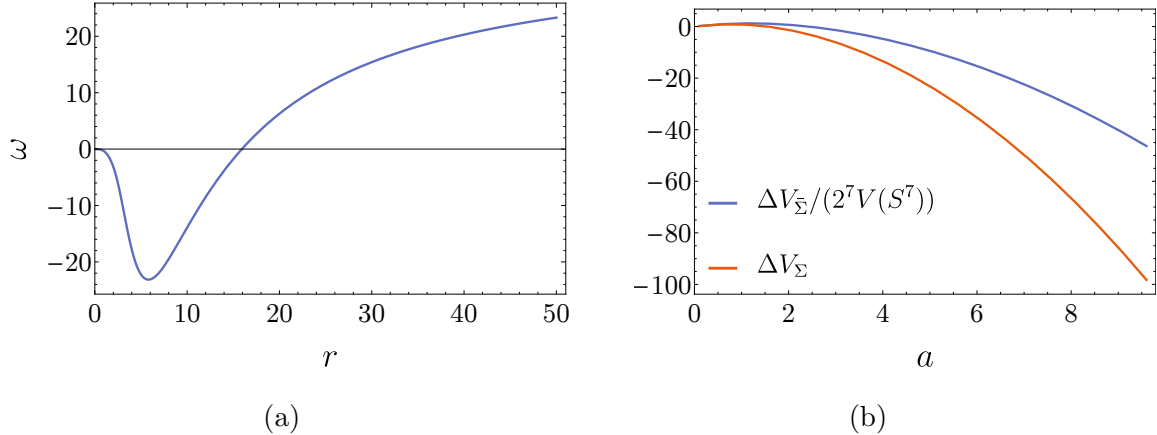


Figure 1. (a) $\omega(r)$ for $a = 5$, and (b) the vacuum-subtracted volume as function of a in units of L .

(which is proven for $d = 3$ [34–36]), which states that⁵

Conjecture 1 ([37]). *Let (Σ, h_0) be a closed hyperbolic Riemannian manifold with constant negative scalar curvature $R[h_0]$. Let h be another metric on Σ with scalar curvature $R[h] \geq R[h_0]$. Then $\text{vol}[\Sigma, h] \geq \text{vol}[\Sigma, h_0]$.*

While this conjecture pertains to compact rather than conformally compact manifolds, there are good reasons to believe it holds for conformally compact manifolds with AdS asymptotics, as discussed in [17]. Now, in our $d = 3$ data the inequality $R[h] \geq R[h_0]$ with h_0 being the metric of hyperbolic space of radius $L = 1$ no longer holds as a consequence of the tachyon condensate, so this is presumably what allows $\mathcal{C}_F < 0$. What about the eleven-dimensional case? Since the WCC allows us to put a lower bound on the intrinsic Ricci scalar of $\tilde{\Sigma}$, it might look like the conditions of Schoen’s theorem hold. But this is not so: the comparison manifold must have a hyperbolic metric h_0 , and static slices of $\text{AdS}_4 \times S^7$ are not hyperbolic. Type IIA, IIB and eleven-dimensional SUGRA all satisfy (see Appendix A.1)⁶

$$t^a t^b \left(R_{ab}[g] - \frac{1}{2} g_{ab} R[g] \right) \geq 0, \quad (2.13)$$

which through the Gauss-Codazzi equation implies that the intrinsic Ricci scalar of any extremal hypersurface in every solution of these theories is positive. Thus, hyperbolic

⁵The conjecture is phrased in a different but equivalent way in [37]. The version stated here can be found in [38].

⁶Thus any AdS vacuum of these theories will satisfy the WCC (1.3) with the relevant AdS radius.

volume comparison theorems no longer apply.⁷ While we do not know of any volume comparison results for asymptotically $\text{AdS}_{d+1} \times K$ type manifolds satisfying (2.13), it is instructive to note that volume comparison results for manifolds of spherical topology tend to imply *lower volume* when the Ricci scalar is higher [38].⁸ This together with our example indicates that, with respect to volume, deformations that mainly affect the compact dimensions behave very different from those that mainly deform the non-compact dimensions.

Finally, let us inquire about the fate of our very low \mathcal{C}_V data upon time-evolution. A guess, in keeping with earlier work on the same tachyonic scalar theory [23] and the spacetimes considered in the next section, would be that it collapses into a big crunch singularity. The negative and unbounded potential $V(\phi) \sim 1 - \cosh \sqrt{2}\phi$ seems to favor such a collapse. However, our data is different from that of [23] and the next section in a significant way: ours has only normalizable modes turned on, so that the ordinary definition of the energy is finite and positive. Furthermore, the source of the decay to a big crunch in [23, 24] was argued to be the presence of a lower unbounded triple trace term in the dual theory Hamiltonian caused by the non-normalizable mode, but here this term is not turned on due to the faster scalar field falloff. It seems likely that our data evolves to eventually form a black hole.

The skeptical reader may at this point refuse to take such unboundedly low \mathcal{C}_F in single-sided spacetimes seriously, pointing out that the CV-proposal was in its original formulation intended to describe wormholes and the volume in the interior of a horizon. Possibly, such a reader may concede, there are some subtleties in one-sided geometries; but surely wormholes – the original motivation for CV – are still safe.

Any such perspective is however about to be disappointed: a small modification of the construction above allows us to build two-boundary geometries supported by tachyonic scalars with unboundedly small vacuum-subtracted volumes. To do so, we modify our construction above by using the following solution to the constraint equations

$$\omega(r) = \frac{1}{2} e^{-\frac{1}{2} \int_{r_0}^r d\rho \rho \phi'(\rho)^2} \left\{ \omega_0 + \int_{r_0}^r d\rho \rho^2 e^{\frac{1}{2} \int_{r_0}^{\rho} dz \phi'(z)^2} \left[(1 + \rho^2) \phi'(\rho)^2 + 2 - 2 \cosh \sqrt{2}\phi \right] \right\}, \quad (2.14)$$

where $1 + r_0^2 - \frac{\omega_0}{r_0} = 0$. For any r_0 we can use a profile similar to (2.11) to make $\text{vol}[\Sigma]$ arbitrarily negative compared to two copies of pure AdS. Thus the phenomenon of lower unbounded \mathcal{C}_F is equally relevant for wormholes.

⁷Strictly speaking they could apply for some choice of h_0 , but not when we pick h_0 to be a solution of the maximal-volume constraints in our theory, which is the relevant case for \mathcal{C}_F .

⁸Note however that in this case, a bound on just the Ricci scalar is not sufficient for volume comparisons. Further bounds on R_{ab} must be satisfied [38].

3 Negatively Divergent \mathcal{C}_F

The clear culprit for negative \mathcal{C}_F in Sec. 2 was compact dimensions or tachyonic scalars. While the main point of interest in this article is the effect of including the compact dimensions, the importance of the scalar tachyons above clearly bears some further investigation. In this section we provide additional examples of tachyonic scalars causing unusual volume behavior. Previous work [26] has conducted a near-boundary analysis that found that turning on boundary sources for these tachyons (thus changing the asymptotic structure, in contrast with the previous section in which the asymptotics were unmodified) can result in initial data that has divergent $\dot{\mathcal{C}}_F$. Our results in this section support this conclusions and expand it further by (1) providing a full spacetime evolution to clarify the physical picture and (2) constructing wormholes with the same properties.

The setting will be unstable asymptotically AdS spacetimes undergoing decay. We will leverage that there are analytical examples of such spacetimes, rather than just initial data. The price we pay is that (1) the theory under consideration does not come from a known realization of AdS/CFT, and (2) the scalar potential is only known numerically. We do not expect this price to be conceptually meaningful: spacetimes that are entirely analogous qualitatively can be constructed numerically directly from the SUGRA potential [23, 24]. Here we prefer to work with an analytically known metric, but we do not expect any of the qualitative features of our analysis to change by the modification of the potential. As emphasized above, we here deviate from the setup of the previous section: the scalar field falloff, which is sufficiently slow that boundary sources are turned on, resulting in a divergent Balasubramanian-Kraus [33] stress tensor. Defining a boundary stress tensor then requires additional counterterms involving the scalar field [23, 39–43]. As we will see, this in turn causes the divergence structure of extremal surface volumes to differ from pure AdS, leading to a UV-divergent \mathcal{C}_F and $\frac{d\mathcal{C}_V}{dt}$.

3.1 AdS Vacuum Decay

The one-sided spacetimes we consider are given by the one-parameter family of metrics constructed in [44], parametrized by the real positive parameter c . These geometries are covered by two coordinate patches, with patch I having metric

$$ds_1^2 = d\xi^2 + a(\xi)^2 (-d\zeta^2 + \cosh^2 \zeta d\Omega^2), \quad (3.1)$$

where $d\Omega^2$ now is the metric of a $d - 1$ -dimensional sphere, and with

$$a(\xi) = (1 + c) \sinh \xi - 2c \sinh \frac{\xi}{2}. \quad (3.2)$$

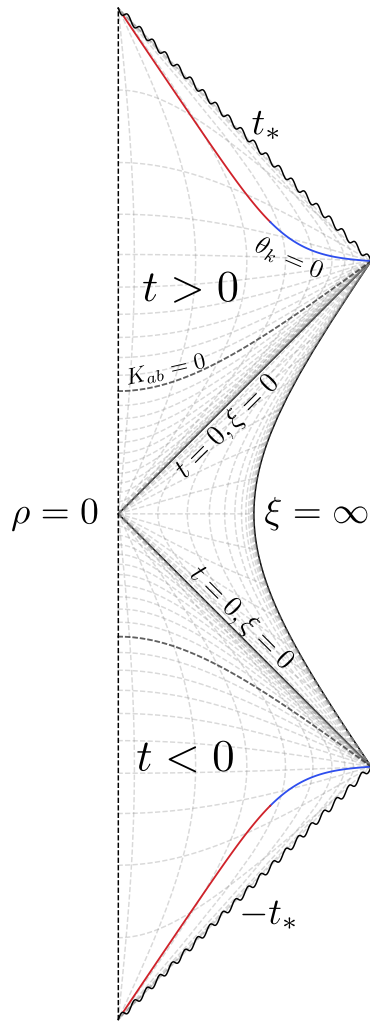


Figure 2. Conformal diagram of the spacetime (3.1) with $d = 3$ and $c = 1$. Dashed lines running vertically are hypersurfaces of constant ρ and ξ , with equidistant coordinate spacing. Dashed lines running horizontally are hypersurfaces of constant t and ζ , with equidistant coordinate spacing. The blue line is the spacelike section of a holographic screen, while the red line is the timelike portion. The darker horizontal dashed lines are the constant $-t$ surfaces at which the FRW region transitions between expanding and crunching ($a'(t) = 0$), which are totally geodesic. These are extremal surface barriers.

The second patch, with coordinates (t, ρ, Ω_i) , is obtained by the analytic continuation $\xi = it, \tau = i\rho$. Patch I is the causal wedge of the spacetime, with the AdS boundary at $\xi = \infty$, where the scalar field is in the false vacuum (a local maximum). As ξ approaches 0, where the edge of the causal wedge lies, the scalar field approaches the true vacuum value. Patch II is an FRW-region which initially expands with motion

away from $t = 0$ and then crunches, with a curvature singularity at $t = \pm t_*$, where $a(it_*) = 0$. Physically, the $\zeta = 0$ slice is a bubble of true vacuum that nucleates inside the false vacuum at a moment of time symmetry. Forward or backward time-evolution results in the subsequent decay of the false AdS vacuum. See Fig. 2 for a conformal diagram drawn for the case $c = 1, d = 3$ (see Appendix A.3 for the computation).

This spacetime has past and future cosmological singularities, and in the boundary conformal frame of the static cylinder, the boundary exists only for a finite time. The dual field theory, if it exists, can either be viewed as living on de Sitter space, or it can be seen as a field theory on the Einstein static universe whose evolution terminates in finite time – possibly due to a Hamiltonian that is unbounded below, as discussed in [23].

\mathcal{C}_F is negative and divergent

Consider again the coordinates

$$ds^2|_{\Sigma} = \frac{1}{1 + r^2 - \frac{\omega(r)}{r^{d-2}}} dr + r^2 d\Omega^2, \quad (3.3)$$

on Σ . Assume now that $\omega(r)$ is divergent at large r , with the leading behavior at large- r given by $\omega(r) \sim \omega_s r^s$ for $0 < s < d$.⁹ The leading ω -dependent divergence in the volume then is given by:

$$\begin{aligned} \text{vol}[\Sigma] &\sim \text{vol}[S^{d-1}] \int^{r_{\text{cut}}} dr \frac{r^{d-1}}{\sqrt{1 + r^2 - \frac{\omega(r)}{r^{d-2}}}} \\ &\sim \text{vol}[S^{d-1}] \int^{r_{\text{cut}}} dr r^{d-2} \left[\frac{1}{2r^{d-s}} \omega_s + \dots \right] \\ &\sim \omega_s \frac{\text{vol}[S^{d-1}] r_{\text{cut}}^{s-1}}{2(s-1)}, \end{aligned} \quad (3.4)$$

Comparing with a slice of pure AdS with cutoff at the same area-radius r_{cut} , we find

$$\text{vol}[\Sigma] - \text{vol}[\Sigma_{\text{AdS}_d}] = \omega_s \frac{\text{vol}[S^{d-1}] r_{\text{cut}}^{s-1}}{2(s-1)} + \text{subleading}. \quad (3.5)$$

We now proceed to show that for our spacetime, we have $s = d - \frac{1}{2}$ and $\omega_s < 0$, giving that \mathcal{C}_F is negative and divergent.

To calculate ω_s , it is useful to know that there is a geometric functional $\omega[\sigma, \Sigma]$ that reduces to $\omega(r)$ when σ is a symmetric codimension-2 spatial surface and Σ spherically

⁹ $s \geq d$ is incompatible with being asymptotically AdS with radius 1.

symmetric [17]:¹⁰

$$\omega[\sigma, \Sigma] = \frac{1}{\text{vol}[S^{d-1}]} \left(\frac{A[\sigma]}{\text{vol}[S^{d-1}]} \right)^{\frac{1}{d-1}} \int_{\sigma} \left[\frac{\mathcal{R}}{(d-1)(d-2)} - \frac{H^2}{(d-1)^2} + \frac{1}{L^2} \right], \quad (3.6)$$

where $H[\sigma]$ is the mean curvature of σ inside Σ and \mathcal{R} the intrinsic Ricci scalar of σ . Let now Σ be the $\zeta = 0$ hypersurface, which is a maximal volume slice since it is a moment of time symmetry. Evaluating $\omega[\sigma, \Sigma]$ for a constant ξ surface σ , we find

$$\omega(\xi) = a(\xi)^{d-2} (1 + a(\xi)^2 - a'(\xi)^2) = -\frac{1}{2^{d-1}} c(1+c)^2 e^{(d-\frac{1}{2})\xi} + \mathcal{O}(e^{(d-1)\xi}). \quad (3.7)$$

If we were to change coordinates to the form (3.3) we would find $r = \mathcal{O}(e^\xi)$, and so indeed we have $s = d - 1/2$, $\omega_s < 0$, showing that \mathcal{C}_F is negative and divergent.

Note that pure AdS-subtracted volume here is somewhat unnatural from the field theory perspective. The scalar field falls off sufficiently slowly so as to turn on a source on the boundary: pure AdS is not a solution of the boundary theory dual to (3.1), so the comparison appears ill-motivated. In this particular setting – though not in the previous section – the negatively divergent \mathcal{C}_F should be viewed as a statement purely about volumes in asymptotically AdS spacetimes, rather than as a statement pertaining to a single field theory. It is in principle possible that the field theory dual to (3.1), if it exists, has a preferred state for the volume subtraction, for which \mathcal{C}_F would be positive.

Complexity change

Let us now compute the leading divergent contribution to the complexity change for spherically symmetric maximal volume slices. To compute the change in complexity we must choose the bulk cutoff carefully. Any given conformal frame induces a unique Fefferman-Graham coordinate system in a neighbourhood of the conformal boundary [45–47]:

$$ds^2 = \frac{1}{z^2} [dz^2 + \gamma_{\mu\nu}(z, x) dx^\mu dx^\nu], \quad (3.8)$$

where $z = 0$ is the conformal boundary and $\gamma_{\mu\nu}(0, x)$ the chosen conformal representative. Given this coordinate system, we can cut off volumes at $z = \epsilon$.

In the case at hand there are two natural conformal frames; we can either choose the boundary to be dS_d or the static cylinder. With respect to the dS_d conformal frame it can readily be checked that the leading divergence in the volume of the maximal volume slice anchored at a constant ζ is

$$\text{vol}[\Sigma_\zeta] = \frac{\text{vol}[S^{d-1}] \cosh \zeta^{d-1}}{(d-1)\epsilon^{d-1}} + \mathcal{O}(\epsilon^{d-3/2}). \quad (3.9)$$

¹⁰This is proportional to the so-called Geroch-Hawking mass when $d = 3$.

This increases to the future and past of $\zeta = 0$ simply because (1) when regulating with a Fefferman-Graham cutoff, the divergence of maximal volume slices is always proportional to the boundary volume in the chosen conformal frame, and (2) the volume of constant ζ slices of de Sitter increases to the future and past.

Next, let us look at the more interesting case of the static cylinder conformal frame. A computation (see appendix A.3) of the leading order complexity change with cutoff adapted to the static cylinder gives

$$\frac{d \text{vol}[\Sigma_t]}{dt} = -\frac{1}{\epsilon^{d-\frac{3}{2}}} \frac{d-1}{d-\frac{3}{2}} \sqrt{\frac{c^2}{2(c+1)}} \frac{\sin t}{(\cos t)^{3/2}} + \mathcal{O}(\epsilon^{-d+2}), \quad t \in \left(-\frac{\pi}{2}, \frac{\pi}{2}\right). \quad (3.10)$$

This is clearly negative and divergent, and so unlike in well known examples of black holes, the moment of time-symmetry is here a maximum of \mathcal{C}_V , rather than a minimum. This is in contrast with the case of the dS conformal frame, and so highlights how extremal hypersurface volume is an observable whose UV-divergence structure depends strongly on the choice of boundary conformal frame. This is consistent with [26]’s near-boundary analysis, which also found a divergent rate of change for tachyonic scalars with boundary sources turned on. In our example we have the additional benefit of knowing the spacetime globally, providing a physical picture of what is happening in the bulk.

The decrease of \mathcal{C}_V is a UV effect, and the volume behind the horizon is admittedly increasing towards the future (before the crunch region that is, which is anyway hidden from all extremal surfaces). However, the volume behind the horizon is not a natural observable to associate to a boundary state at a fixed time, since turning on sources in the future would alter the horizon location, and thus also the volume behind it. Nevertheless, it does seem that the CV proposal needs some modification in the spacetimes considered in this section. One possibility is some generalized volume functional that includes contributions from the scalar fields, which from a dimensional reduction perspective this appears natural.

3.2 Decaying Cosmological Wormholes

Can we find a wormhole with the same properties as the spacetime considered above – a wormhole with cosmological singularities, negative divergent complexity of formation, and decreasing late time complexity? That would appear to be in some tension with the paradigm of wormhole volume corresponding to increasing complexity; such an example would add urgency in finding an appropriate modification of CV that can accommodate such spacetimes.

It turns out that we can, in fact, build such a spacetime. The procedure is borrowed from [48, 49], which constructs a two-boundary wormhole from a single-sided

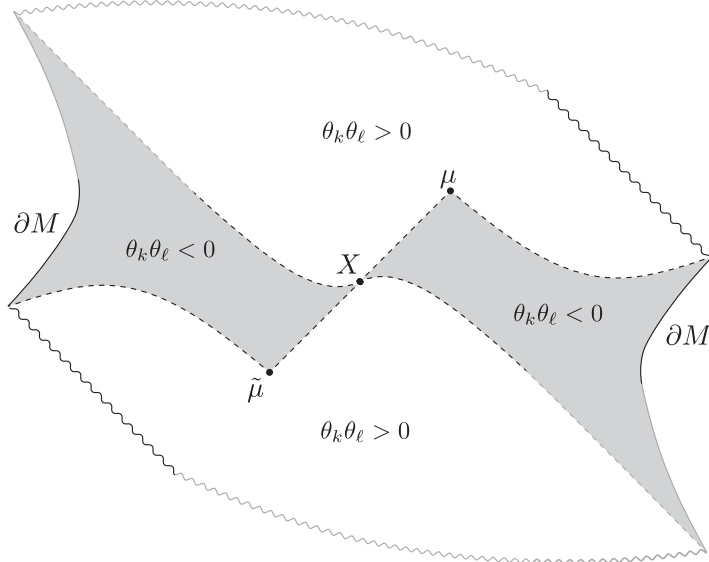


Figure 3. Black lines show numerically computed features of a coarse-grained spacetime formed from a marginally trapped (minimar [48]) surface μ on the spacelike section of the holographic screen shown Fig. 2. Dashed lines represent apparent horizons, while X is the HRT surface. Grey lines lie outside the range of our numerics, and are pure sketches representing a qualitative image of how the full spacetime could look like. For an illustration with additional details, see Fig. 4 in the appendix.

spacetime containing a marginally trapped surface satisfying certain assumptions. The protocol is roughly as follows: one fixes the data in the exterior of a given marginally trapped surface μ ; the rest of the initial data is provided on a stationary null hypersurface fired towards the past interior from μ . This hypersurface eventually develops an extremal surface on it; at this surface, the initial data is CPT conjugated, resulting in a second boundary. The initial data is characteristic; in our case, fixing a spherically symmetric marginally trapped surface means that obtaining the spacetime requires numerical evolution of the spherically symmetric characteristic Einstein-Klein-Gordon equations. We will not expound on the details of the numerics here (although they are surprisingly simple), instead just briefly summarizing our results. Figure 3 illustrates one of these wormholes. On the left, we show the marginally trapped surface μ used to build the wormhole embedded in the original spacetime. On the left we see the coarse-grained spacetime in the regions where we are able to obtain it numerically. We have not obtained any parts of the spacetime in the future or past of X , since this requires evolution past a shockwave, requiring more sophisticated methods than our fairly straightforward technique. The upshot of this solution is that spacetime emergence connecting two asymptotic boundaries via an interior need *not* feature a simple

complexity growth with time, emphasizing the necessity of a refinement to the Complexity=Volume proposal that takes into account the different behaviors of deformed theories. We emphasize that this is qualitatively (as well as quantitatively) different from the negative \mathcal{C}_F of the previous section, in which no boundary sources were turned on.

Acknowledgments

It is a pleasure to thank Jan de Boer, Shira Chapman, Sebastian Fischetti, Patrick Jefferson, Lampros Lamprou, Hong Liu, Dan Roberts, and Wati Taylor for discussions. This work is supported in part by NSF grant no. PHY-2011905 and the MIT department of physics. The work of NE was also supported in part by the U.S. Department of Energy, Office of Science, Office of High Energy Physics of U.S. Department of Energy under grant Contract Number DE-SC0012567 (High Energy Theory research) and by the U.S. Department of Energy Early Career Award DE-SC0021886. The work of ÅF is also supported in part by an Aker Scholarship.

A Appendix

A.1 The DEC and SEC in type II and $D = 11$ SUGRA

The DEC and the SEC for p -forms

Consider a stress tensor

$$T_{ab} = \frac{1}{p!} \left[p F_a{}^{c_2 \dots c_p} F_{bc_2 \dots c_p} - \frac{k}{2} g_{ab} F^{c_1 \dots c_p} F_{c_1 \dots c_p} \right], \quad 1 \leq k \leq p, \quad (\text{A.1})$$

where $F_{c_1 \dots c_p}$ is a p -form. For $k = 1$ this is just the stress tensor of a free $(p - 1)$ form with curvature $F_{c_1 \dots c_p}$ and action $S = -\frac{1}{2} \int F \wedge \star F$. We first check the DEC. Let u^a, v^b be any two timelike vectors at a point p . We will normalize them to our convenience, since the DEC is independent of the choice of normalization. Choose Riemann normal coordinates at q , so that $g_{\mu\nu}|_q = \eta_{\mu\nu}$ and $u^\mu = (\partial_t)^\mu$, where $\eta_{\mu\nu}$ is the Minkowski metric in Cartesian coordinates. Next, we can always rescale v and perform a rotation of our coordinates so that

$$v^\mu = (\partial_t)^\mu + f(\partial_x)^\mu, \quad (\text{A.2})$$

for some constant $f \geq 0$. With this, we now find at q that

$$v^a u^b T_{ab} = T_{tt} + f T_{tx}. \quad (\text{A.3})$$

We compute that

$$\begin{aligned}
p!T_{tt} &= \sum_{\mu_i} \left(pF_t^{\mu_2 \dots \mu_p} F_{t\mu_2 \dots \mu_p} + \frac{k}{2} F^{\mu_1 \dots \mu_p} F_{\mu_1 \dots \mu_p} \right) \\
&= \left(p - \frac{k}{2} \right) \sum_{\mu_i} F_{t\mu_2 \dots \mu_p}^2 + \frac{k}{2} \sum_{\mu_i, \mu_1 \neq t} F_{\mu_1 \dots \mu_p}^2 \\
&\geq \left(p - \frac{k}{2} \right) \sum_{\mu_i} F_{t\mu_2 \dots \mu_p}^2 + \frac{k}{2} \sum_{\mu_i} F_{x\mu_2 \dots \mu_p}^2,
\end{aligned} \tag{A.4}$$

and

$$p!T_{tx} = \sum_{\mu_i} pF_t^{\mu_2 \dots \mu_p} F_{x\mu_2 \dots \mu_p} = p \sum_{\mu_i} F_{t\mu_2 \dots \mu_p} F_{x\mu_2 \dots \mu_p}. \tag{A.5}$$

And so adding up (A.4) and (A.5) we get

$$\begin{aligned}
p!T_{ab}u^a v^b &\geq p \sum_{\mu_i} \left[\left(1 - \frac{k}{2p} \right) F_{t\mu_2 \dots \mu_p}^2 + \frac{1}{2} f F_{t\mu_2 \dots \mu_p} F_{x\mu_2 \dots \mu_p} + \frac{k}{2} F_{x\mu_2 \dots \mu_p}^2 \right] \\
&\quad + \frac{1}{2} p f \sum_{\mu_i} F_{t\mu_2 \dots \mu_p} F_{x\mu_2 \dots \mu_p} \\
&\geq p \sum_{\mu_i} \left[\left(1 - \frac{k}{2p} \right) F_{t\mu_2 \dots \mu_p}^2 + \frac{1}{2} f F_{t\mu_2 \dots \mu_p} F_{x\mu_2 \dots \mu_p} + \frac{k}{2} F_{x\mu_2 \dots \mu_p}^2 \right].
\end{aligned} \tag{A.6}$$

This is non-negative for each term in the sum. If $F_{t\mu_2 \dots \mu_p} F_{x\mu_2 \dots \mu_p} \geq 0$ this is obvious, since we assumed $1 \leq k \leq p$, giving that each term is manifestly non-negative. So assume $F_{t\mu_2 \dots \mu_p} F_{x\mu_2 \dots \mu_p} < 0$. In this case we get a smaller term if we replace (1) $f \rightarrow 2$, (2) $k \rightarrow p$ in the first term, and (3) $k \rightarrow 1$ in the last term:

$$p!T_{ab}u^a v^b \geq p \sum_{\mu_i} \left[\frac{1}{2} F_{t\mu_2 \dots \mu_p}^2 + F_{t\mu_2 \dots \mu_p} F_{x\mu_2 \dots \mu_p} + \frac{1}{2} F_{x\mu_2 \dots \mu_p}^2 \right] \geq 0. \tag{A.7}$$

Thus the DEC holds for the stress tensor (A.1). Together with $G_{ab} = 8\pi G_N T_{ab}$, this implies the WCC (1.3).

Next, let us turn to the SEC. Set $8\pi G_N = 1$. Then

$$T \equiv T^a_a = g^{ab} G_{ab} = (1 - D/2) R \tag{A.8}$$

and so

$$R_{ab} t^a t^b = \left(G_{ab} + \frac{1}{2} g_{ab} R \right) t^a t^b = T_{ab} t^a t^b - \frac{1}{2} R = T_{ab} t^a t^b - \frac{1}{2 - D} T. \tag{A.9}$$

Our stress tensor gives

$$p!T = \frac{1}{2} (2p - kD) F^{c_1 \dots c_p} F_{c_1 \dots c_p}. \quad (\text{A.10})$$

Choosing again Riemann normal coordinates at our point of interest, we get

$$\begin{aligned} p!R_{\mu\nu}t^\mu t^\nu &= \left(p - \frac{k}{2}\right) \sum_{\mu_i} F_{t\mu_2 \dots \mu_p}^2 + \frac{k}{2} \sum_{\mu_i, \mu_1 \neq t} F_{\mu_1 \dots \mu_p}^2 - \frac{1}{2} \frac{2p - kD}{2 - D} F_{\mu_1 \dots \mu_p} F^{\mu_1 \dots \mu_p} \\ &\geq \left(p - \frac{k}{2} - \frac{1}{2} \frac{kD - 2p}{D - 2}\right) \sum_{\mu_i} F_{t\mu_2 \dots \mu_p}^2 \\ &\geq \left(p - \frac{p}{2} - \frac{1}{2} \frac{pD - 2p}{D - 2}\right) \sum_{\mu_i} F_{t\mu_2 \dots \mu_p}^2 \\ &= 0, \end{aligned}$$

where we used that $1 \leq k \leq p$ above. Thus the SEC holds for the stress tensor (A.1).

Type IIB

From [50, 51] we have that the gravitational equations of motion of the bosonic sector of type IIB supergravity in the Einstein frame can be written as

$$\begin{aligned} R_{ab} &= \frac{1}{2} \nabla_a \phi \nabla_b \phi + \frac{1}{2} e^{2\phi} \nabla_a \chi \nabla_b \chi + \frac{1}{96} H_{acdef} H_b{}^{cdef} + \frac{1}{4} e^{-\phi} \left[F_{acd} F_b{}^{cd} - \frac{1}{12} g_{ab} F_{cde} F^{cde} \right] \\ &\quad + \frac{1}{4} e^{-\phi} \left[L_{acd} L_b{}^{cd} - \frac{1}{12} g_{ab} L_{cde} L^{cde} \right] \end{aligned} \quad (\text{A.11})$$

where H is a five form and F and L are three-forms. The scalar stress tensors are (up to a positive rescaling in the case of χ) just stress tensors of massless scalars and so satisfies the DEC and the SEC. Thus we just need to check that the p -forms. Rewriting the equation in Einstein form we get stress tensors

$$\begin{aligned} T_{ab}^{(H)} &= \frac{1}{5 \times 96} \left(5 H_{acdef} H_b{}^{cdef} - \frac{5}{2} g_{ab} H_{cdefg} H^{cdefg} \right) \\ T_{ab}^{(F)} &= \frac{1}{12} e^{-\phi} \left(3 F_{acd} F_b{}^{cd} - \frac{1}{2} g_{ab} F_{cde} F^{cde} \right) \\ T_{ab}^{(L)} &= \frac{1}{12} e^{\phi} \left(3 L_{acd} L_b{}^{cd} - \frac{1}{2} g_{ab} L_{cde} L^{cde} \right) \end{aligned} \quad (\text{A.12})$$

All of these stress tensors are proportional to (A.1) with a positive coefficient, and so the DEC and SEC holds.

Type IIA and $D = 11$ supergravity

In the Einstein frame, the stress tensors of the bosonic matter in type IIA and eleven-dimensional supergravity is just that of free p -form fields, except for an overall positive factor proportional to an exponential of the dilaton in the case of type IIA [52]. The exact kind of computation as was carried out above shows that the WEC holds classically in these theories.

A.2 General properties of $K = 0$ slices in SUGRA

We here derive and highlight some general results on slices of vanishing mean curvature in type IIA/B and $D = 11$ SUGRA. This will justify our statement that the initial data in Sec. 2 gives the unique maximal volume slice in the evolved spacetime.

The first observation is the following:

Proposition 1. *The bosonic matter fields of type IIA, IIB and $D = 11$ supergravity in the Einstein frame satisfies the strong energy condition (SEC) and the dominant energy condition (DEC):*

$$\begin{aligned} \text{SEC:} \quad & T_{ab}u^a u^b + \frac{1}{D-2}T^a_a \geq 0, & \forall \text{timelike } u^a, \\ \text{DEC:} \quad & T_{ab}u^a v^a \geq 0, & \forall \text{timelike } u^a, v^a. \end{aligned} \tag{A.13}$$

This result is known in the literature [53–55], but for convenience we included a derivation above, as the result is often stated without proof. Note that this result applies to the standard bosonic fields, and does not include stringy curvature corrections or additional massive fields. Also, dimensional reduction will in general both break the SEC [55] and the DEC [21] (although for specific types of compactifications they might survive [54]).

The well known fact that the SEC combined with $K = 0$ implies maximality [56, 57] now immediately gives

Proposition 2. *Let (M, g) be any classical solution of type IIA, IIB, or $D = 11$ SUGRA in the Einstein frame. If Σ is a $K = 0$ spacelike hypersurface, possibly with boundary, then Σ is maximal under any variation that leaves its boundary fixed.*

This is a manifestation of the well known fact that the SEC ensures focusing of timelike congruences. The result follows from calculating the second variation of the volume of a spacelike $K = 0$ hypersurface, which reads [56, 57]

$$\delta^2 \text{vol}[\Sigma] = - \int_{\Sigma} (|DN|^2 + N^2 K_{ab} K^{ab} + N^2 R_{ab} n^a n^a) \leq 0, \tag{A.14}$$

where τ^a is the vector field generating the variation of Σ , n^a a unit normal to Σ , D_a the connection on Σ , and $N = \tau \cdot n$. It is assumed that the boundary of Σ is kept fixed in (A.14).

As described above, Proposition 2 will generally not be true in dimensionally reduced spacetime, and so in this case we actually have better control in the full $D = 10, 11$ spacetime. This shows a situation in AdS/CFT where the compact dimensions should be viewed as a resource rather than a nuisance.

Next, [58] has showed that if the SEC holds, then there cannot be two $K = 0$ slices anchored at the same boundary time in an asymptotically AdS spacetime (the proof survives when we also have a compact space). Thus we have the result

Proposition 3. *Let (M, g) be an asymptotically $AdS_{d+1} \times X$ solution of type IIA, IIB, or $D = 11$ SUGRA in the Einstein frame for some compact manifold X . Let Σ be a complete maximal volume slice anchored at boundary time C . Then there is no other maximal volume slice in the domain of dependence of Σ that is anchored at C .*

Proposition 2 and 3 now justifies our assertion from Sec. 2 that our initial data Σ is the true maximal volume slice.

Finally, we remark that Proposition 2 and 3 remain true if we add additional SEC-respecting matter, such p -dimensional branes B with action

$$S = - \int_B d^p x \sqrt{-h} T + \int_B C_p, \quad (\text{A.15})$$

where T is a non-negative potentially field-dependent scalar and C_p a p -form – both independent of the induced metric h_{ab} on B .

A.3 AdS Vacuum Decay Computations

Kruskal coordinates

Define

$$\hat{a}(t) = a(it) = (1 + c) \sin t - 2c \sin \frac{t}{2}. \quad (\text{A.16})$$

Consider the metric (3.1) in the special case of $c = 1$ and $d = 3$. Define the functions

$$R(\xi) = \int_{\xi_0}^{\xi} \frac{d\xi'}{a(\xi')} = \frac{1}{3} \log \left[\frac{f(\xi)}{f(\xi_0)} \right], \quad T(t) = \int_{t_0}^t \frac{dt'}{\hat{a}(t')} = \frac{1}{3} \log \left[\frac{\hat{f}(t)}{\hat{f}(t_0)} \right] \quad (\text{A.17})$$

where

$$f(\xi) = \frac{\cosh\left(\frac{\xi}{4}\right) \sinh\left(\frac{\xi}{4}\right)^3}{\left(1 - 2 \cosh\left(\frac{\xi}{2}\right)\right)^2} = \begin{cases} \frac{\xi^3}{64} + \mathcal{O}(\xi^5) & \xi \ll 1 \\ \frac{1}{16} - \frac{3}{16}e^{-\xi} - \frac{1}{8}e^{-3\xi/2} + \mathcal{O}(e^{-2\xi}) & \xi \gg 1 \end{cases} \quad (\text{A.18})$$

$$\hat{f}(t) = \frac{\cos\left(\frac{t}{4}\right) \sin\left(\frac{t}{4}\right)^3}{\left(1 - 2 \cos\left(\frac{t}{2}\right)\right)^2} = \begin{cases} \frac{t^3}{64} + \mathcal{O}(t^5) & t \ll 1 \\ \frac{1}{4\sqrt{3}(t_* - t)^2} - \frac{1}{8(t_* - t)} + \mathcal{O}(1) & t_* - t \ll 1 \end{cases}$$

where $t_* = \frac{2\pi}{3}$ is the location of the future singularity, ie. the maximal value of t . The constants $t_0 > 0$ and $\xi_0 > 0$ will be chosen later. We have $T \in \mathbb{R}$ with $T = \infty$ the future singularity and $T = -\infty$ the future event horizon, so the coordinate T covers only the future FRW region. We have $R \in (-\infty, R_\partial)$ where $R = -\infty$ is the event horizon and R_∂ the conformal boundary. Define now Kruskal coordinates

$$U = \begin{cases} e^{T(t)-\rho} & \text{Region II} \\ -e^{-\zeta+R(\xi)} & \text{Region I} \end{cases} \quad V = \begin{cases} e^{T(t)+\rho} & \text{Region II} \\ e^{\zeta+R(\xi)} & \text{Region I} \end{cases}. \quad (\text{A.19})$$

where we now take Region II temporarily to mean the future part only. This gives

$$T(U, V) = \frac{1}{2} \log(UV), \quad \rho(U, V) = \frac{1}{2} \log(V/U), \quad U > 0, \quad (\text{A.20})$$

$$\zeta(U, V) = \frac{1}{2} \log(-V/U), \quad R(U, V) = \frac{1}{2} \log(-VU), \quad U < 0. \quad (\text{A.21})$$

The future event horizon is now at $U = 0$ and the past event horizon at $V = 0$. The octant $V \geq U \geq 0$ covers the future part of of region I, with $\rho = 0$ at $U = V$. The singularity lies at $(U > 0, V = \infty)$. The conformal boundary is at $VU = -e^{2R_\partial}$, and region I is covered by the regions $U \leq 0$ and $0 \leq V \leq -\frac{e^{2R_\partial}}{U}$.

Let us now define the functions

$$\hat{t}(X) = T^{-1}\left(\frac{1}{2} \log X\right), \quad \hat{\xi}(X) = R^{-1}\left(\frac{1}{2} \log(-X)\right), \quad (\text{A.22})$$

so that $t(U, V) = \hat{t}(UV)$ and $\xi(U, V) = \hat{\xi}(UV)$. The domain of \hat{t} is $X \in (0, \infty)$. Since $R \in (-\infty, R_{\max})$, we have that the domain of $\hat{\xi}$ is $X \in (-e^{2R_{\max}}, 0)$. Finally changing the coordinates, we find that the metric is

$$ds^2 = b(UV) \left[-dUdV + \left(\frac{V-U}{2}\right)^2 d\Omega^2 \right], \quad (\text{A.23})$$

where

$$b(UV) = \begin{cases} \frac{\hat{a}(\hat{t}(UV))^2}{\sqrt{U^2V^2}}, & U > 0, V > 0, \\ \frac{\hat{a}(\hat{\xi}(UV))^2}{\sqrt{U^2V^2}}, & U < 0, V > 0. \end{cases} \quad (\text{A.24})$$

Note that the inverse functions T^{-1} and R^{-1} must be computed numerically, and so the same is also true of b .

In order for $b(X)$ to be continuous at $X = 0$ we need to choose ξ_0, t_0 appropriately. For small arguments we have

$$\begin{aligned}\frac{\log(-UV)}{2} &= R(\xi) = \log\left(\frac{\xi}{4}\right) - \frac{1}{3}\log f(\xi_0) + \mathcal{O}(\xi^2), \\ \frac{\log UV}{2} &= T(t) = \log\left(\frac{t}{4}\right) - \frac{1}{3}\log \hat{f}(t_0) + \mathcal{O}(t^2),\end{aligned}\tag{A.25}$$

which at small t and ξ gives the relation

$$\begin{aligned}\xi &= 4f(\xi_0)^{1/3}\sqrt{-UV}, \\ t &= 4\hat{f}(t_0)^{1/3}\sqrt{UV}.\end{aligned}\tag{A.26}$$

Now, near the horizon we have that $\hat{a}(t) = t + \dots$ and $a(\xi) = \xi + \dots$, so the function b near the horizon reads

$$b(UV) = \begin{cases} 16\hat{f}(t_0)^{2/3} + \dots \\ 16f(\xi_0)^{2/3} + \dots \end{cases}.\tag{A.27}$$

Thus, continuity of b requires t_0 and ξ_0 to be related by

$$f(\xi_0) = \hat{f}(t_0).\tag{A.28}$$

The conformal diagram

The metric (A.23) is just conformal to Minkowski, and so drawing the conformal diagram is just as for Minkowski, with two exceptions:

- In the region of negative U , $-UV \geq e^{2R\partial}$ is excised since it lies beyond the conformal boundary.
- The part which corresponds to null infinity in Minkowski (and which is not in the excised region) is here instead a singularity at a finite proper distance.

From these observations, we easily find Fig. 2. In our representation have chosen $t_0 = 1$ and rescaled the null coordinates by a convenient overall factor in order to bring the holographic screen closer to the center of the diagram.

The holographic screen

Consider the radial null vectors

$$k^a = \frac{1}{\sqrt{2}\hat{a}(t)} \left[(\partial_t)^a + \frac{1}{\hat{a}(t)} (\partial_\rho)^a \right], \quad \ell^a = \frac{\hat{a}(t)}{\sqrt{2}} \left[(\partial_t)^a - \frac{1}{\hat{a}(t)} (\partial_\rho)^a \right],\tag{A.29}$$

which are normalized so that $k \cdot \ell = -1$ and so that $k^a \nabla_a k^b = 0$. Calculating the expansions, we find

$$\begin{aligned}\theta_k &= \frac{\sqrt{2}}{\hat{a}(t)^2} \left(\hat{a}'(t) + \frac{1}{\tanh \rho} \right) \\ \theta_\ell &= -\sqrt{2} \left(-\hat{a}'(t) + \frac{1}{\tanh \rho} \right)\end{aligned}\tag{A.30}$$

For times where $\hat{a}'(t) < -1$, we have marginally trapped surfaces at

$$\rho(t) = \operatorname{arctanh} \left(-\frac{1}{\hat{a}'(t)} \right).\tag{A.31}$$

The unnormalized tangents to the screen that are orthogonal to the marginally trapped leaves are

$$\eta^a = (\partial_t)^a + \rho'(t)(\partial_\rho)^a = (\partial_t)^a + \frac{\hat{a}''(t)}{1 - \hat{a}'(t)^2}(\partial_\rho)^a.\tag{A.32}$$

Its norm is given by

$$\eta^2 = -1 + \frac{\hat{a}(t)^2 \hat{a}''(t)^2}{(\hat{a}'(t)^2 - 1)^2},\tag{A.33}$$

which starts out being positive and then transitions to negative at late times.

Timelike geodesics must cross the horizon

Consider a timelike geodesic in region II, which by spherical symmetry can be taken to lie at $\theta = \pi/2$ without loss of generality. The effective Lagrangian for a geodesic is

$$\mathcal{L} = g_{\mu\nu} u^\mu u^\nu = \dot{\xi}^2 - a(\xi)^2 \dot{\zeta}^2 + a(\xi)^2 \cosh^2 \zeta \dot{\varphi}^2,\tag{A.34}$$

Parametrizing by proper time, so that $\mathcal{L} = -1$, gives

$$-\dot{\zeta}^2 + \cosh^2 \zeta \dot{\varphi}^2 = -\frac{1 + \dot{\xi}^2}{a^2}.\tag{A.35}$$

Then the geodesic equation for ξ can then be written

$$0 = \ddot{\xi} - aa' \left(-\dot{\zeta}^2 + \cosh^2 \zeta \dot{\varphi}^2 \right) = \ddot{\xi} + \frac{a'}{a} (1 + \dot{\xi}^2).\tag{A.36}$$

Interestingly the angular momentum makes no presence here, so there is no angular moment barrier between the horizon and the conformal boundary. Since $a'(\xi)/a(\xi) > 1$ everywhere, this equation effectively describes a particle subject to friction and a force always pushing in the direction of negative ξ . Thus no geodesic can avoid reaching $\xi = 0$. After this, it enters region II, where it is doomed to encounter the singularity in finite time. Thus, every timelike geodesic ends up in the singularity, and so the singularity is rightfully described as cosmological.

Computing $\dot{\mathcal{C}}_V$

Let us consider the static cylinder conformal frame. Defining $\xi = -\log z$, the metric in the causal wedge becomes

$$\begin{aligned} ds_I^2 &= \frac{1}{z^2} [dz^2 + f(z)^2 (d\zeta^2 + \cosh^2 \zeta d\Omega^2)] \\ f(z) &= \frac{[1-z][1+c(\sqrt{z}-1)^2+z]}{2} = \frac{1+c}{2} - c\sqrt{z} + \mathcal{O}(z). \end{aligned} \quad (\text{A.37})$$

Next we introduce new coordinates (w, t) through:

$$\begin{aligned} \zeta &= 2 \operatorname{arctanh} \left(\tan \frac{t}{2} \right), \\ z &= w \frac{c+1}{2 \cos t}. \end{aligned} \quad (\text{A.38})$$

To subleading order in w , this transforms the metric into Fefferman-Graham coordinates of the static cylinder:

$$\begin{aligned} ds_I^2 &= \frac{1}{w^2} [dw^2 + h(w, t)^2 (-dt^2 + d\Omega^2) + \mathcal{O}(w)], \\ h(w, t) &= 1 - \sqrt{w} \sqrt{\frac{2c^2}{(c+1) \cos t}}, \end{aligned} \quad (\text{A.39})$$

where t lies in the finite range $|t| < \pi/2$. Consider now a hypersurface Σ_{t_0} with embedding coordinates $(w, t(w), \Omega_i)$, and where $t(0) = t_0$. Its volume reads

$$\operatorname{vol}[\Sigma_{t_0}] = \operatorname{vol}[S^{d-1}] \int dw \frac{h(w, t)^{d-1}}{w^d} \sqrt{1 - h(w, t)t'(w)^2}. \quad (\text{A.40})$$

Expanding near the boundary,

$$t(w) = t_0 + t_1 w + \mathcal{O}(w^{3/2}), \quad (\text{A.41})$$

we find that extremality imposes $t_1 = 0$. Consequentially, the divergence of the volume to subleading order is

$$\begin{aligned} \operatorname{vol}[\Sigma_{t_0}] &= \operatorname{vol}[S^{d-1}] \int_{\epsilon} dw \left(w^{-d} - w^{-d+1/2}(d-1) \sqrt{\frac{2c^2}{(c+1) \cos t_0}} + \mathcal{O}(w^{-d+1}) \right) \\ &= \operatorname{vol}[S^{d-1}] \left[\frac{1}{(d-1)} \epsilon^{-d+1} - \frac{d-1}{d-\frac{3}{2}} \epsilon^{-d+\frac{3}{2}} \sqrt{\frac{2c^2}{(c+1) \cos t_0}} + \mathcal{O}(\epsilon^{-d+2}) \right]. \end{aligned} \quad (\text{A.42})$$

This implies that the leading order complexity change with cutoff adapted to the static cylinder is given by (3.10).

Plot of the Cosmological Wormhole

Fig. 4 shows the domain for which the numerical determination of the coarse grained spacetime has been carried out, together with data on null expansions and area–radii in the geometry.

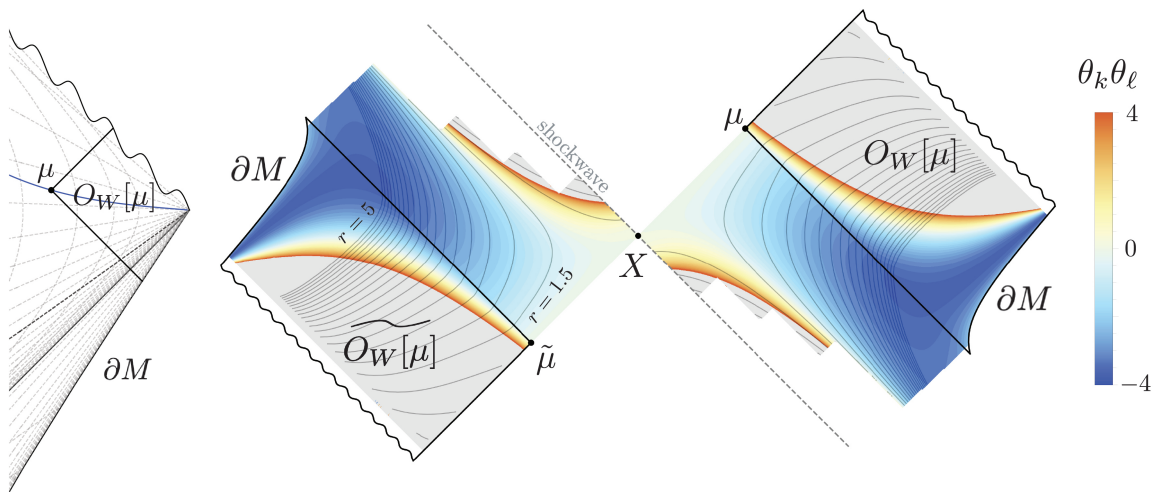


Figure 4. To the left, we have zoomed into the outer wedge $O_W[\mu]$ of a marginally trapped surface μ on the spacelike section of the holographic screen in Fig. 2. On the right, we show the coarse-grained spacetime corresponding to μ in the regions where we have been able to obtain the metric numerically. The black contour lines show surfaces of constant area radius, saturating at $r = 5$ and with spacings of $\delta r \approx 0.2$. The colored contours show the product of the null expansions $\theta_k \theta_\ell$ for constant $-r$ surfaces, with gray regions corresponding to $\theta_k \theta_\ell > 4$. The shockwave passing through the HRT surface X carries no null energy, but does source a discontinuity in the inaffinity of ℓ^a , which is the null vector along the direction of the shockwave. The quantity $\ell^a \nabla_a \phi$ is discontinuous at X .

References

- [1] S. Ryu and T. Takayanagi, *Holographic derivation of entanglement entropy from AdS/CFT*, *Phys.Rev.Lett.* **96** (2006) 181602, [[hep-th/0603001](#)].
- [2] S. Ryu and T. Takayanagi, *Aspects of Holographic Entanglement Entropy*, *JHEP* **0608** (2006) 045, [[hep-th/0605073](#)].

- [3] V. E. Hubeny, M. Rangamani, and T. Takayanagi, *A Covariant holographic entanglement entropy proposal*, *JHEP* **0707** (2007) 062, [[arXiv:0705.0016](#)].
- [4] A. C. Wall, *Maximin Surfaces, and the Strong Subadditivity of the Covariant Holographic Entanglement Entropy*, *Class.Quant.Grav.* **31** (2014), no. 22 225007, [[arXiv:1211.3494](#)].
- [5] B. Czech, J. L. Karczmarek, F. Nogueira, and M. Van Raamsdonk, *The Gravity Dual of a Density Matrix*, *Class.Quant.Grav.* **29** (2012) 155009, [[arXiv:1204.1330](#)].
- [6] T. Faulkner, A. Lewkowycz, and J. Maldacena, *Quantum corrections to holographic entanglement entropy*, *JHEP* **1311** (2013) 074, [[arXiv:1307.2892](#)].
- [7] A. Lewkowycz and J. Maldacena, *Generalized gravitational entropy*, *JHEP* **1308** (2013) 090, [[arXiv:1304.4926](#)].
- [8] X. Dong, *Holographic Entanglement Entropy for General Higher Derivative Gravity*, *JHEP* **01** (2014) 044, [[arXiv:1310.5713](#)].
- [9] J. Maldacena and L. Susskind, *Cool horizons for entangled black holes*, [arXiv:1306.0533](#).
- [10] N. Engelhardt and A. C. Wall, *Quantum Extremal Surfaces: Holographic Entanglement Entropy beyond the Classical Regime*, *JHEP* **01** (2015) 073, [[arXiv:1408.3203](#)].
- [11] L. Susskind, *Computational Complexity and Black Hole Horizons*, *Fortsch. Phys.* **64** (2016) 24–43, [[arXiv:1403.5695](#)]. [Addendum: *Fortsch.Phys.* 64, 44–48 (2016)].
- [12] D. Stanford and L. Susskind, *Complexity and Shock Wave Geometries*, *Phys. Rev. D* **90** (2014), no. 12 126007, [[arXiv:1406.2678](#)].
- [13] A. R. Brown, D. A. Roberts, L. Susskind, B. Swingle, and Y. Zhao, *Holographic Complexity Equals Bulk Action?*, *Phys. Rev. Lett.* **116** (2016), no. 19 191301, [[arXiv:1509.07876](#)].
- [14] A. R. Brown, D. A. Roberts, L. Susskind, B. Swingle, and Y. Zhao, *Complexity, action, and black holes*, *Phys. Rev. D* **93** (2016), no. 8 086006, [[arXiv:1512.04993](#)].
- [15] D. L. Jafferis, A. Lewkowycz, J. Maldacena, and S. J. Suh, *Relative entropy equals bulk relative entropy*, [arXiv:1512.06431](#).
- [16] X. Dong, *The Gravity Dual of Renyi Entropy*, *Nature Commun.* **7** (2016) 12472, [[arXiv:1601.06788](#)].
- [17] N. Engelhardt and Å. Folkestad, *General Bounds on Holographic Complexity*, [arXiv:2109.06883](#).
- [18] S. Chapman, H. Marrochio, and R. C. Myers, *Complexity of Formation in Holography*, *JHEP* **01** (2017) 062, [[arXiv:1610.08063](#)].

- [19] S. Chapman, D. Ge, and G. Policastro, *Holographic Complexity for Defects Distinguishes Action from Volume*, *JHEP* **05** (2019) 049, [[arXiv:1811.12549](#)].
- [20] A. Bernamonti, F. Galli, J. Hernandez, R. C. Myers, S.-M. Ruan, and J. Simón, *Aspects of The First Law of Complexity*, [arXiv:2002.05779](#).
- [21] T. Hertog, G. T. Horowitz, and K. Maeda, *Negative energy density in Calabi-Yau compactifications*, *JHEP* **05** (2003) 060, [[hep-th/0304199](#)].
- [22] P. Breitenlohner and D. Z. Freedman, *Positive energy in anti-de Sitter backgrounds AND gauged extended supergravity*, *Phys. Lett.* **B115** (1982) 197.
- [23] T. Hertog and G. T. Horowitz, *Towards a big crunch dual*, *JHEP* **07** (2004) 073, [[hep-th/0406134](#)].
- [24] T. Hertog and G. T. Horowitz, *Holographic description of AdS cosmologies*, *JHEP* **04** (2005) 005, [[hep-th/0503071](#)].
- [25] S. Fischetti, D. Marolf, and A. C. Wall, *A paucity of bulk entangling surfaces: AdS wormholes with de Sitter interiors*, *Class.Quant.Grav.* **32** (2015), no. 6 065011, [[arXiv:1409.6754](#)].
- [26] M. Moosa, *Divergences in the rate of complexification*, *Phys. Rev. D* **97** (2018), no. 10 106016, [[arXiv:1712.07137](#)].
- [27] A. Belin, A. Lewkowycz, and G. Sárosi, *Complexity and the bulk volume, a new York time story*, *JHEP* **03** (2019) 044, [[arXiv:1811.03097](#)].
- [28] N. Chagnet, S. Chapman, J. de Boer, and C. Zukowski, *Complexity for Conformal Field Theories in General Dimensions*, [arXiv:2103.06920](#).
- [29] M. Flory and M. P. Heller, *Geometry of Complexity in Conformal Field Theory*, *Phys. Rev. Res.* **2** (2020), no. 4 043438, [[arXiv:2005.02415](#)].
- [30] M. Flory and M. P. Heller, *Conformal field theory complexity from Euler-Arnold equations*, *JHEP* **12** (2020) 091, [[arXiv:2007.11555](#)].
- [31] M. Cvetič, M. J. Duff, P. Hoxha, J. T. Liu, H. Lu, J. X. Lu, R. Martinez-Acosta, C. N. Pope, H. Sati, and T. A. Tran, *Embedding AdS black holes in ten-dimensions and eleven-dimensions*, *Nucl. Phys. B* **558** (1999) 96–126, [[hep-th/9903214](#)].
- [32] D. Marolf, O. Parrikar, C. Rabideau, A. Izadi Rad, and M. Van Raamsdonk, *From Euclidean Sources to Lorentzian Spacetimes in Holographic Conformal Field Theories*, *JHEP* **06** (2018) 077, [[arXiv:1709.10101](#)].
- [33] V. Balasubramanian and P. Kraus, *A Stress tensor for Anti-de Sitter gravity*, *Commun. Math. Phys.* **208** (1999) 413–428, [[hep-th/9902121](#)].
- [34] G. Perelman, *The entropy formula for the Ricci flow and its geometric applications*, *arXiv Mathematics e-prints* (Nov., 2002) math/0211159, [[math/0211159](#)].

- [35] G. Perelman, *Ricci flow with surgery on three-manifolds*, *arXiv Mathematics e-prints* (Mar., 2003) math/0303109, [[math/0303109](#)].
- [36] I. Agol, N. M. Dunfield, P. A. Storm, and W. P. Thurston, *Lower bounds on volumes of hyperbolic Haken 3-manifolds*, *arXiv Mathematics e-prints* (June, 2005) math/0506338, [[math/0506338](#)].
- [37] R. M. Schoen, *Variational theory for the total scalar curvature functional for riemannian metrics and related topics*, in *Topics in Calculus of Variations* (M. Giaquinta, ed.), (Berlin, Heidelberg), pp. 120–154, Springer Berlin Heidelberg, 1989.
- [38] H. L. Bray, *The Penrose inequality in general relativity and volume comparison theorems involving scalar curvature*. PhD thesis, STANFORD UNIVERSITY, Nov., 1997.
- [39] M. Henneaux, C. Martinez, R. Troncoso, and J. Zanelli, *Black holes and asymptotics of 2+1 gravity coupled to a scalar field*, *Phys. Rev. D* **65** (2002) 104007, [[hep-th/0201170](#)].
- [40] G. T. Horowitz, *Creating naked singularities and negative energy*, *Phys. Scripta T* **117** (2005) 86–91, [[hep-th/0312123](#)].
- [41] M. Henneaux, C. Martinez, R. Troncoso, and J. Zanelli, *Asymptotically anti-de Sitter spacetimes and scalar fields with a logarithmic branch*, *Phys. Rev. D* **70** (2004) 044034, [[hep-th/0404236](#)].
- [42] T. Hertog and K. Maeda, *Black holes with scalar hair and asymptotics in $N = 8$ supergravity*, *JHEP* **07** (2004) 051, [[hep-th/0404261](#)].
- [43] M. Henneaux, C. Martinez, R. Troncoso, and J. Zanelli, *Asymptotic behavior and Hamiltonian analysis of anti-de Sitter gravity coupled to scalar fields*, *Annals Phys.* **322** (2007) 824–848, [[hep-th/0603185](#)].
- [44] X. Dong and D. Harlow, *Analytic Coleman-De Luccia Geometries*, *JCAP* **1111** (2011) 044, [[arXiv:1109.0011](#)].
- [45] C. Fefferman and C. R. Graham, *Conformal invariants*, *Elie Cartan et les Mathématiques d’aujourd’hui* (Astérisque) p. 95. 1985.
- [46] C. Graham and J. M. Lee, *Einstein metrics with prescribed conformal infinity on the ball*, *Advances in Mathematics* **87** (1991), no. 2 186–225.
- [47] C. R. Graham and E. Witten, *Conformal anomaly of submanifold observables in AdS / CFT correspondence*, *Nucl. Phys. B* **546** (1999) 52–64, [[hep-th/9901021](#)].
- [48] N. Engelhardt and A. C. Wall, *Coarse Graining Holographic Black Holes*, *JHEP* **05** (2019) 160, [[arXiv:1806.01281](#)].

- [49] N. Engelhardt and A. C. Wall, *Decoding the Apparent Horizon: Coarse-Grained Holographic Entropy*, *Phys. Rev. Lett.* **121** (2018), no. 21 211301, [[arXiv:1706.02038](#)].
- [50] H. Lu, C. N. Pope, and T. A. Tran, *Five-dimensional $N=4$, $SU(2) \times U(1)$ gauged supergravity from type IIB*, *Phys. Lett. B* **475** (2000) 261–268, [[hep-th/9909203](#)].
- [51] D. Cassani, G. Dall’Agata, and A. F. Faedo, *Type IIB supergravity on squashed Sasaki-Einstein manifolds*, *JHEP* **05** (2010) 094, [[arXiv:1003.4283](#)].
- [52] M. J. D. Hamilton, *The field and Killing spinor equations of M-theory and type IIA/IIB supergravity in coordinate-free notation*, [arXiv:1607.00327](#).
- [53] J. M. Maldacena and C. Nunez, *Supergravity description of field theories on curved manifolds and a no go theorem*, *Int. J. Mod. Phys. A* **16** (2001) 822–855, [[hep-th/0007018](#)].
- [54] G. W. Gibbons, *Thoughts on tachyon cosmology*, *Class. Quant. Grav.* **20** (2003) S321–S346, [[hep-th/0301117](#)].
- [55] P. K. Townsend and M. N. R. Wohlfarth, *Accelerating cosmologies from compactification*, *Phys. Rev. Lett.* **91** (2003) 061302, [[hep-th/0303097](#)].
- [56] D. Brill and F. Flaherty, *Isolated maximal surfaces in spacetime*, *Communications in Mathematical Physics* **50** (1976), no. 2 157–165.
- [57] J. E. Marsden and F. J. Tipler, *Maximal hypersurfaces and foliations of constant mean curvature in general relativity*, *Physics Reports* **66** (1980), no. 3 109–139.
- [58] J. Couch, S. Eccles, T. Jacobson, and P. Nguyen, *Holographic Complexity and Volume*, *JHEP* **11** (2018) 044, [[arXiv:1807.02186](#)].